

Age-Related Changes in Trabecular Architecture Differ in Female and Male C57BL/6J Mice*

Vaida Glatt,¹ Ernesto Canalis,² Lisa Stadmeier,² and Mary L Bouxsein¹

ABSTRACT: We used μ CT and histomorphometry to assess age-related changes in bone architecture in male and female C57BL/6J mice. Deterioration in vertebral and femoral trabecular microarchitecture begins early, continues throughout life, is more pronounced at the femoral metaphysis than in the vertebrae, and is greater in females than males.

Introduction: Despite widespread use of mice in the study of musculoskeletal disease, the age-related changes in murine bone structure and the relationship to whole body BMD changes are not well characterized. Thus, we assessed age-related changes in body composition, whole body BMD, and trabecular and cortical microarchitecture at axial and appendicular sites in mice.

Materials and Methods: Peripheral DXA was used to assess body composition and whole body BMD in vivo, and μ CT and histomorphometry were used to measure trabecular and cortical architecture in excised femora, tibia, and vertebrae in male and female C57BL/6J mice at eight time-points between 1 and 20 mo of age ($n = 6$ –9/group).

Results: Body weight and total body BMD increased with age in male and female, with a marked increase in body fat between 6 and 12 mo of age. In contrast, trabecular bone volume (BV/TV) was greatest at 6–8 wk of age and declined steadily thereafter, particularly in the metaphyseal region of long bones. Age-related declines in BV/TV were greater in female than male. Trabecular bone loss was characterized by a rapid decrease in trabecular number between 2 and 6 mo of age, and a more gradual decline thereafter, whereas trabecular thickness increased slowly over life. Cortical thickness increased markedly from 1 to 3 mo of age and was maintained or slightly decreased thereafter.

Conclusions: In C57BL/6J mice, despite increasing body weight and total body BMD, age-related declines in vertebral and distal femoral trabecular bone volume occur early and continue throughout life and are more pronounced in females than males. Awareness of these age-related changes in bone morphology are critical for interpreting the skeletal response to pharmacologic interventions or genetic manipulation in mice.

J Bone Miner Res 2007;22:1197–1207. Published online on May 7, 2007; doi: 10.1359/JBMR.070507

Key words: murine, trabecular bone, aging, microarchitecture

INTRODUCTION

ANIMAL MODELS ARE commonly used in the study of skeletal biology and serve as useful tools to delineate mechanisms underlying bone loss and skeletal fragility. In animals and humans, a bone mass measurement in adulthood reflects the amount of bone achieved during the period of peak bone mass acquisition, and the subsequent decline caused by both aging and gonadal insufficiency. Whereas ovariectomized rodents have been

widely used to explore skeletal changes after estrogen deficiency, models for studying the age-related bone changes in gonadally intact animals are less common. Moreover, despite widespread use of mice in biological studies of musculoskeletal disease, there have been few studies that have characterized the age-related changes in murine bone structure.

Most previous studies of age-related changes in murine bone characterized changes in cortical bone structure and indicated that cortical thickness decreases and cross-sectional moment of inertia increases with increasing age.^(1–5) In addition, total femoral volumetric BMD (vBMD), which reflects mainly the cortical bone compartment, increases until 4 mo of age and is maintained thereafter.⁽⁶⁾ However, little is known about age-related changes in murine trabecular microarchitecture, with one

*Presented in part at the Orthopaedic Research Society Annual Meeting, Chicago, IL, USA, March 19–22, 2006, and the 28th Annual Meeting of the American Society for Bone and Mineral Research, Philadelphia, PA, USA, September 15–19, 2006.

The authors state that they have no conflicts of interest.

¹Orthopedic Biomechanics Laboratory, Beth Israel Deaconess Medical Center and Harvard Medical School, Boston, Massachusetts, USA; ²Department of Research, Saint Francis Hospital and Medical Center, Hartford, Connecticut, USA.

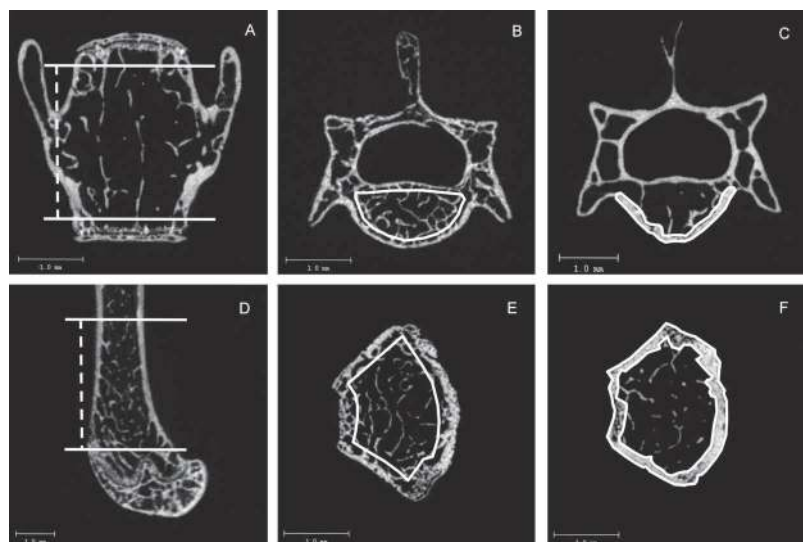


FIG. 1. 2D μ CT images showing regions of trabecular bone evaluation in the (A and B) lumbar vertebrae and (D and E) distal femur, along with example of how cortical bone region was outlined in the (C) vertebral body and (F) distal femur.

study reporting early and progressive decline in trabecular bone volume at the proximal tibia in male mice.⁽⁷⁾

Additional data are needed to characterize the age-related changes in trabecular bone morphology in mice, including the timing of “peak” bone mass and whether males and females show similar age-related changes in trabecular and cortical bone. Therefore, the objectives of the current study were to assess age- and sex-related changes in body composition, whole body BMD, histomorphometric indices of trabecular bone morphology and turnover, and 3D indices of trabecular microarchitecture in the axial and appendicular skeleton. We also determined whether age-related changes in trabecular bone were accompanied by alterations in bone cross-sectional geometry and cortical thickness.

MATERIALS AND METHODS

Animals

Male and female C57BL/6J inbred mice were obtained from the Jackson Laboratory, maintained under standard conditions, and killed at 1, 1.5, 2, 3, 4, 6, 12, and 20 mo of age for assessment of bone morphology by μ CT ($n = 6$ –9 per age and per sex). For histomorphometry, different cohorts of male and female mice were killed at 1, 3, 5, and 12 mo of age ($n = 3$ –11 per age and sex). Animals were housed four mice per cage and were maintained on a 12:12-h light-dark cycle with access to mouse chow (TD8664; Harlan Teklad, Indianapolis, IN, USA) containing 2.5% calcium and 1.2% phosphorus. The animal protocol was approved by the ethical committees on animal care and use at Beth Israel Deaconess Medical Center, Boston, MA, and at St Francis Hospital and Medical Center, Hartford, CT.

Body composition and total body BMD

We measured total body BMD (g/cm^2), total body BMC (g), and total body fat (%) by peripheral DXA (PIXImus2;

GE Lunar, Madison, WI, USA) at 1, 2, 3, 4, 6, and 12 mo of age ($n = 7$ –26 per group), as previously described.⁽⁸⁾ Some mice were assessed longitudinally, whereas others were assessed at a single time-point. Because of the body size limitation on DXA, it was not possible to collect data on 20-mo-old mice.

Bone architecture by μ CT

At the time of death, mice were weighed, and the right femur, tibia, and fifth lumbar vertebral body (L_5) were dissected, cleaned of soft tissue, and stored in 70% ethanol. Femoral length was measured to the nearest 0.01 mm using digital calipers. μ CT (μ CT40; Scanco Medical AG, Basserdorf, Switzerland) was used to assess trabecular bone morphology in the fifth lumbar vertebrae (L_5), distal femoral metaphysis, and proximal tibial metaphysis using a 12- μm isotropic voxel size, as previously described.^(8,9) Previous studies have reported skeletal site differences in patterns of bone loss in inbred mouse strains^(8,10); therefore, we chose to assess both an axial (i.e., the vertebral body) and appendicular (i.e., the distal femur and proximal tibia) site for trabecular architecture. Moreover, these are the sites most commonly used in skeletal biology studies in mice. Because age- and sex-specific patterns of bone architecture changes were nearly identical at the proximal tibia and distal femur, we report data for the distal femur.

For L_5 , transverse μ CT slices were acquired for the entire vertebral body, and trabecular bone was evaluated in a region 0.3 mm below the cranial and above the caudal growth plate regions (Fig. 1A). For the distal femur, transverse CT slices were evaluated in the region starting 360 μm proximal to the growth plate and extending 1800 μm proximally (Fig. 1D). For younger mice (i.e., 4 and 6 wk of age), the location and length of the region of interest was adjusted in proportion to vertebral height and femoral length. In all cases, the trabecular bone region was identified manually by tracing the region of interest (Figs. 1B and 1E). Images were thresholded using an adaptive-iterative algorithm,^(11–13)

and morphometric variables were computed from the binarized images using direct, 3D techniques that do not rely on any prior assumptions about the underlying structure.^(14–16) For trabecular bone regions, we assessed the bone volume fraction (BV/TV, %), trabecular thickness (Tb.Th, μm), trabecular number (Tb.N, mm^{-1}), trabecular separation (Tb.Sp, μm), connectivity density (ConnD, $1/\text{mm}^3$), and structure model index (SMI).

To measure cross-sectional area (CSA, mm^2) of the vertebral body, we used the μCT images to delineate a region of interest around the entire vertebral body at four locations along the height of the vertebrae and computed the average CSA. Vertebral cortical thickness was computed by manually delineating the ventral vertebral cortex for 100 slices of the cranial vertebral body (Fig. 1C). CSA and cortical thickness at the distal femur (Fig. 1F) were assessed for the same set of slices used to assess trabecular bone properties. For both the vertebral body and distal femur, cortical thickness was determined using the distance-transform method.⁽¹⁵⁾

Bone histomorphometric analysis

Static and dynamic histomorphometry was carried out on femurs from 1-, 3-, 5-, and 12-mo-old male and female mice. Mice were injected with calcein, 20 mg/kg, and demeclocycline, 50 mg/kg, at intervals of 2–7 days, depending on their age, and killed by CO_2 inhalation. Femurs were dissected, fixed in 70% ethanol, dehydrated, and embedded undecalcified in methyl methacrylate. Longitudinal sections, 5 μm thick, were cut on a Microm microtome (Richard-Allan Scientific, Kalamazoo, MI, USA) and stained with 0.1% toluidine blue, pH 6.4, or von Kossa. Static parameters of bone formation and resorption were measured in a defined area between 725 and 1270 μm from the growth plate, using an OsteoMeasure morphometry system (Osteometrics, Atlanta, GA, USA). For dynamic histomorphometry, mineralizing surface per bone surface (MS/BS, %) and mineral apposition rate (MAR, $\mu\text{m}/\text{d}$) were measured in unstained sections under UV light and used to calculate bone formation rate with a surface referent (BFR, $\mu\text{m}^3/\mu\text{m}^2/\text{d}$), as previously described.⁽¹⁷⁾ We also measured the eroded surface per bone surface (ES/BS, %) and number of osteoblasts (NOB/BPm, mm^{-1}) and osteoclasts (NOC/BPm, mm^{-1}) per bone perimeter. The terminology and units used are those recommended by the Histomorphometry Nomenclature Committee of the American Society for Bone and Mineral Research.⁽¹⁸⁾

Data analysis

Standard descriptive statistics were computed, and data were checked for normality. Two-way ANOVA was used to assess the overall influence of age and sex on skeletal morphology. Unpaired *t*-tests were used to evaluate differences between sexes at each age. The percent change in each parameter over life was computed between 2 and 20 mo using a regression model, derived from the mean values at each age. Both linear and nonlinear relationships were

tested, and the best fitting model was used for analysis of age-related changes. All tests were two-tailed, with differences considered significant at $p < 0.05$. Data are presented as mean \pm SE, unless otherwise noted.

RESULTS

Age-related changes in body composition, femur length, and total body BMD

Body weight increased 3-fold over life, from 16.3 ± 0.9 to 45.7 ± 2.6 g in males and from 11.6 ± 0.7 to 35.6 ± 1.6 g in females (Fig. 2A). Femoral length increased rapidly until 3 mo of age, more slowly until 6 mo of age, and plateaued thereafter (Fig. 2B). As expected, compared with females, males were significantly heavier at all time-points and had increased femoral length, except at 12 and 20 mo. In both sexes, total body BMD (TBBMD) increased steadily with age (Fig. 2C), whereas body fat, expressed as a percent of total body weight, was constant until 6 mo of age and increased markedly between 6 and 12 mo of age (Fig. 2D). Accordingly, the percent lean mass was steady until 6 mo of age and declined markedly from 6 to 12 mo of age (data not shown). females tended to have higher percent fat (Fig. 2D) and lower lean mass than males. The patterns of age-related changes in body weight, femur length, total body BMD, and body composition did not differ between males and females.

Age-related changes in trabecular bone architecture by μCT

Age-related changes in trabecular bone architecture are shown in Figs. 3 and 4. Vertebral trabecular BV/TV increased between 1 and 2 mo in males and females and declined thereafter in females. In males, BV/TV was stable until 6 mo and declined. Overall, there was a greater decline in BV/TV over life in females than males (52% versus 26%, $p = 0.05$; Table 1; Fig. 3A), and females had lower vertebral BV/TV than males throughout life ($p < 0.01$). ANOVA revealed a significant age-by-sex interaction among adults, indicating that patterns of age-related change differed in males and females. In both sexes, vertebral Tb.N peaked at 1–2 mo of age and declined thereafter, with a greater decline over life in females than males (Table 1; Fig. 3C). Tb.N was lower in females than males at all ages ($p < 0.01$). In contrast, vertebral Tb.Th increased steadily until 4 mo in both sexes and plateaued in males, while continuing to increase slightly in females with age (Table 1; Fig. 3E). Connectivity density declined similarly with age in both sexes and was lower at all ages in females than males (Fig. 3G). From 1 to 2 mo, vertebral trabecular SMI declined, indicative of a shift to a more platelike architecture, and was relatively constant thereafter in both sexes (Fig. 3I).

Age-related changes in trabecular architecture at the distal femur followed similar patterns as the vertebrae, although the decline in BV/TV over life was more dramatic, particularly in females at early ages (Figs. 3 and 4). At the distal femur, trabecular BV/TV peaked between 1 and 2 mo

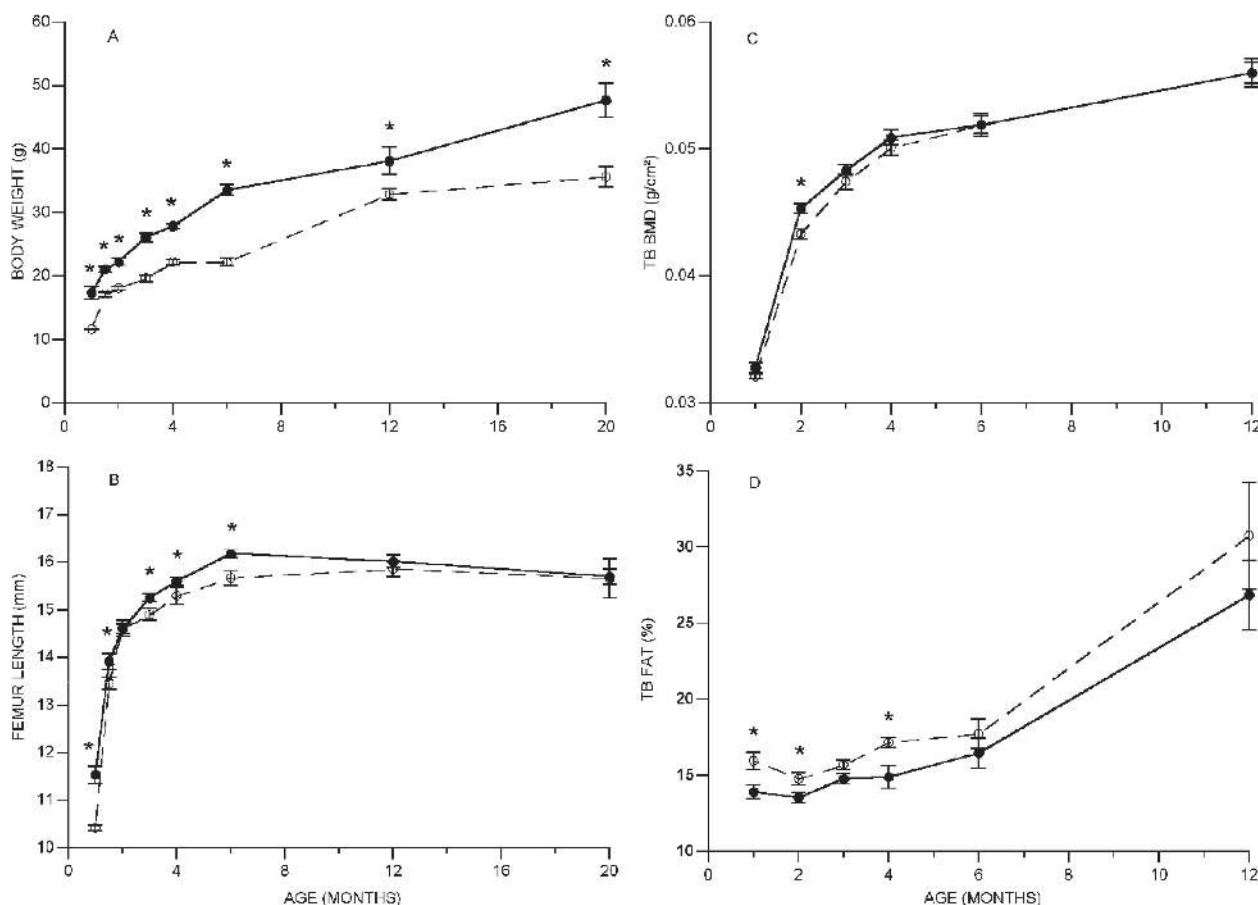


FIG. 2. Changes in body composition, femoral length, and whole body BMD in male and female mice from 1 to 20 mo of age (mean \pm SE). Males are represented by solid symbol and line, whereas females are shown as open symbol and dashed line. *Difference between males and females at a given age ($p < 0.05$).

of age and declined thereafter, with a greater decline in females than males over life (-94% versus -56% , respectively; $p < 0.05$; Table 1; Fig. 3B). Generally, females had lower BV/TV than males, particularly at the oldest age ($1.0 \pm 0.3\%$ versus $10.7 \pm 1.3\%$ in females and males, respectively; $p < 0.001$). Tb.N at the distal femur showed a similar pattern as BV/TV, increasing between 1 and 2 mo of age and declining thereafter, with males having higher values than females (Fig. 3D). With aging, Tb.Th increased slightly in both males and females (Fig. 3F). In males, SMI changed little with age, whereas in females, it increased markedly between 1 and 3 mo of age and plateaued (Fig. 3J), resulting in a higher SMI (i.e., more rodlike structure) throughout life for female mice ($p < 0.001$ versus males). Age-related changes in trabecular architecture at the proximal tibia followed similar patterns as the distal femur (data not shown).

Age-related changes in bone CSA and cortical thickness by μ CT

To evaluate potential concomitant changes in bone size or cortical properties, we assessed CSA and cortical bone morphology (Table 1; Fig. 5). At both the vertebral body

and distal femur, there was a marked increase in CSA during the rapid growth phase, but thereafter, no notable age-related changes (Fig. 5). females had greater vertebral CSA than males at 12 and 18 mo (Fig. 5A), whereas males had higher CSA of the distal femur at most time-points. In both males and females, thickness of the ventral vertebral cortex increased markedly from 1 to 3 mo of age and was maintained or slightly increased thereafter. At the distal femur, cortical thickness increased dramatically from 1 to 3 mo of age and was maintained or declined slightly, yet was generally higher in females than males (Fig. 5D).

Age-related changes in bone structure and remodeling indices by histomorphometry

To assess potential cellular mechanisms underlying the age-related changes, we assessed static and dynamic indices of bone structure and turnover by histomorphometric analysis of the distal femoral metaphysis in male and female mice at 1, 3, 5, and 12 mo of age (Fig. 6). Similar to μ CT findings, trabecular BV/TV declined steadily with age in both sexes, but more rapidly in female than male mice ($p < 0.01$; Fig. 6A). The decline in BV/TV was accompanied by

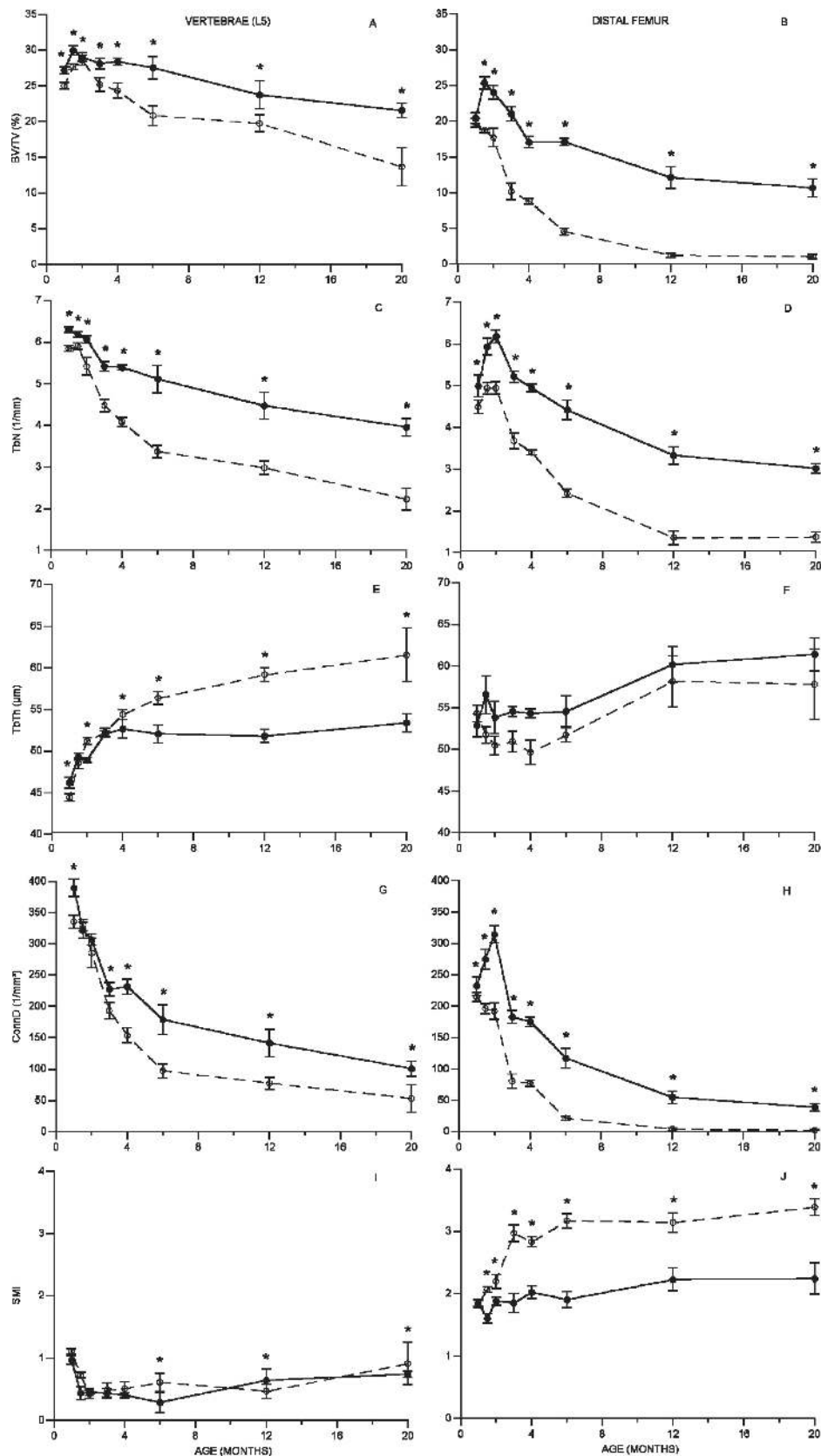


FIG. 3. Changes in trabecular bone architecture at the fifth lumbar vertebral body and distal femoral metaphysis in male and female C57Bl/6J mice from 1 to 20 mo of age, assessed by μ CT (mean \pm SE). Males are represented by solid symbol and line, whereas females are shown as open symbol and dashed line. *Difference between males and females at a given age ($p < 0.05$).

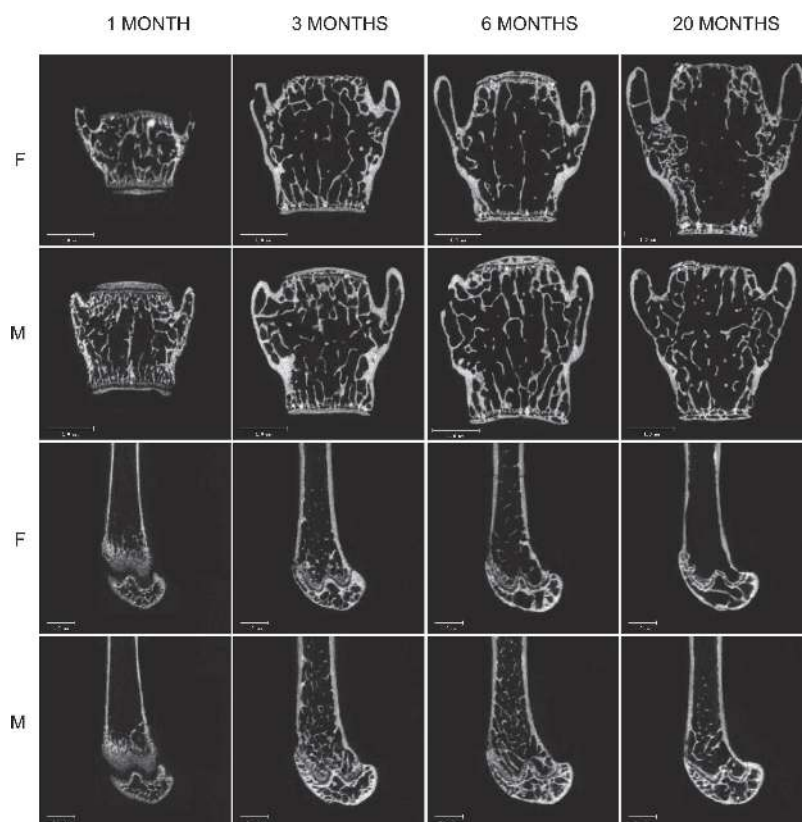


FIG. 4. Representative 2D μ CT images showing age-related changes in trabecular bone architectures in male and female mice at the lumbar spine (L_5) and distal femur.

decreased trabecular number ($p < 0.001$), along with maintained or increased trabecular thickness (Fig. 6). Consistent with an overall increase in bone turnover, the extent of mineralizing surface increased in both sexes with age ($p = 0.016$). In males, MAR declined from 1 to 3 mo ($p < 0.005$) and was maintained thereafter, whereas it was unchanged in females. Accordingly, there was no net change in BFR with age in either sex. ES/BS declined significantly from 1 to 3 mo ($p < 0.01$), increased from 3 to 5 mo ($p < 0.05$), and either remained stable (in males) or declined again (in females). ES/BS was similar in males and females, except at 5 mo of age, where it was 46% higher in females ($p = 0.04$). The number of osteoblasts declined 2- to 3-fold from 1 to 3 mo of age ($p < 0.01$ for both males and females), and was constant thereafter (Fig. 6H). The number of osteoclasts also declined from 1 to 3 mo ($p < 0.001$) but increased at 5 mo, particularly in females ($p < 0.01$), before declining again at 12 mo ($p < 0.01$; Fig. 6I). The number of osteoclasts and osteoblasts was significantly higher in females than males (overall $p < 0.001$).

DISCUSSION

We found that, whereas body weight and whole body BMD increase steadily throughout life, trabecular bone volume fraction is greatest at a relatively young age and declines steadily thereafter in C57BL/6J mice. The age-related

deterioration in trabecular bone architecture was more severe in the metaphyseal region of the long bones than the vertebral body. Finally, we noted in separate groups of animals evaluated by different techniques, namely 3D μ CT and 2D histomorphometry, that age-related changes in trabecular bone occur earlier and are more dramatic in female than male mice, particularly in the secondary spongiosa region of the distal femur.

Our data indicating that trabecular bone volume peaks at an early age and declines thereafter are consistent with a prior study of trabecular architecture in the proximal tibia of male C57BL/6 mice.⁽⁷⁾ The early decline in BV/TV is caused primarily by a decrease in trabecular number and is accompanied by an age-related increase in trabecular thickness, particularly in the long bones, a phenomena also seen by Halloran et al.⁽⁷⁾ The decline in trabecular number may result from remodeling activity that attempts to create a more efficient, organized structure according to the predominant loading conditions,⁽¹⁹⁾ whereas the increase in mean trabecular thickness may represent a compensatory thickening of existing trabeculae as thinner ones are resorbed, and stress on existing trabeculae increases. Alternatively, the increase in mean trabecular thickness may reflect the phenomenon that, as thinner trabeculae are removed, the average thickness of remaining trabeculae increases. If the increase in trabecular thickness was caused primarily by resorption of thin trabeculae, one would expect that the SD of trabecular thickness measurements

TABLE 1. BONE MICROARCHITECTURE AT THE LUMBAR SPINE AND DISTAL FEMUR, ASSESSED BY μ CT

| | Females | | Males | | <i>p</i> | |
|-------------------------------|--------------------------|---------------------------------|--------------------------|---------------------------------|---|---|
| | Mean \pm SE at 2 mo | Percent change over life* | Mean \pm SE at 2 mo | Percent change over life* | Male vs. female difference at 2 mo [†] | Male vs. female difference in age-related change [‡] |
| Lumbar spine | | | | | | |
| BV/TV (%) | 28.6 \pm 0.7 | -52% | 29.1 \pm 0.6 | -26% | NS | 0.0578 |
| TbTh (μ m) | 51.2 \pm 0.4 | 20% | 48.9 \pm 0.3 | 9% | 0.0005 | 0.0005 |
| TbSp (μ m) | 179 \pm 7 | 168% | 155 \pm 2 | 56% | 0.0039 | 0.0001 |
| TbN (mm^{-1}) | 5.4 \pm 0.2 | -59% | 6.1 \pm 0.1 | -35% | 0.0097 | 0.0252 |
| ConnD ($1/\text{mm}^3$) | 286 \pm 24 | -81% | 306 \pm 9 | -67% | NS | NS |
| SMI | 0.42 \pm 0.07 | 118% | 0.46 \pm 0.06 | 63% | NS | NS |
| CSA (mm^2) | 1.72 \pm 0.06 | 25% | 1.63 \pm 0.02 | 10% | NS | 0.0001 |
| Cortical thickness (μ m) | 85 \pm 2 | 8% | 77 \pm 1 | 22% | 0.0048 | NS |
| Distal femur | | | | | | |
| BV/TV (%) | 17.7 \pm 1.3 | -94% | 24.1 \pm 0.9 | -56% | 0.0008 | 0.02 |
| TbTh (μ m) | 50.5 \pm 1.1 | 3% | 53.8 \pm 1.9 | 14% | NS | NS |
| TbSp (μ m) | 196 \pm 7 | 281% | 153 \pm 4 | 110% | 0.0001 | 0.0001 |
| TbN (mm^{-1}) | 4.9 \pm 0.1 | -72% | 6.2 \pm 0.2 | -51% | 0.0001 | NS |
| ConnD ($1/\text{mm}^3$) | 192 \pm 12 | -99% | 314 \pm 14 | -88% | 0.0007 | 0.0002 |
| SMI | 2.19 \pm 0.11 | 54% | 1.88 \pm 0.07 | 19% | 0.0537 | 0.0041 |
| CSA (mm^2) | 3.21 \pm 0.15 | -3% | 3.40 \pm 0.04 | -5% | NS | NS |
| Cortical thickness (μ m) | 121 \pm 2 | -4% | 100 \pm 3 | 19% | 0.0002 | 0.0062 |

* Computed from regression of mean values between 2 and 20 mo of age, expressed as percent change from 2 to 20 mo.

[†] *p* value determined from unpaired Student's *t*-test.

[‡] *p* value of age-by-sex interaction term in ANOVA, ages 2–20 mo.

BV/TV, bone volume/tissue volume; Tb.N, trabecular number; Tb.Th, trabecular thickness; Tb.Sp, trabecular separation; ConnD, connectivity density; SMI, structure model index; CSA, cross-sectional area.

(Tb.Th.SD) would decrease with age. However, our data indicate that the SD of trabecular thickness measurements (Tb.Th.SD) is either constant or increases slightly with increasing age (data not shown), thus providing partial support for the view that thickness of individual trabeculae may increase in a compensatory fashion driven by mechanical loading.

We found that age-related changes in trabecular bone architecture follow slightly different patterns in female than male mice. Females tended to undergo a more rapid decline in BV/TV in adolescence, whereas rates of decline were similar in adulthood, although perhaps slightly delayed in males compared with females. The mechanisms underlying these age-related changes in trabecular bone in the absence of gonadal insufficiency are incompletely understood. The decline in gonadal steroid production with age may contribute to some of the changes we observed. Serum estradiol peaks at 2 mo of age in females, at levels three to five times higher than in males, and declines gradually thereafter (in both sexes), remaining higher in females throughout life.^(20–22) In comparison, testosterone is 20-fold higher in male than female mice, and whereas females show little age-related change, in males, values decline 3- to 4-fold from 6 to 12 mo of age, still remaining markedly higher than females at all ages.^(20–22) The higher androgen levels in males may provide partial protection from age-related decline in trabecular bone.⁽²³⁾

With increased age, expression patterns of RANKL and OPG tend to favor osteoclast over osteoblast activity.⁽²⁴⁾

Aging also significantly increases stromal/osteoblastic cell-induced osteoclastogenesis, promotes expansion of the osteoclast precursor pool, and alters the relationship between osteoblasts and osteoclasts in cancellous bone.⁽²⁵⁾ Several factors may contribute to this altered balance between osteoclast and osteoblast activity with increased age, including age-related altered hormonal and cytokine profiles,^(5,26) increased oxidative stress,^(27,28) declines in physical activity,⁽⁵⁾ alterations in body composition, and marrow adiposity.^(29–33)

We observed that, in both sexes, the decline in trabecular bone volume occurred at the same time that total body BMD and total body fat were increasing. This indicates that total body BMD is relatively insensitive to changes in the trabecular compartment. The pattern of increase in total body BMD with age was similar to the pattern for femoral length, consistent with the view that the total body BMD measurement reflects increases in bone size, as well as bone acquisition in the cortical compartment. The early, rapid decline in BV/TV occurred when body fat was reasonably stable; however, the subsequent decline in BV/TV during adulthood occurred while body fat increased markedly. It may be that the increase in total body fat was subsequent to a decline in physical activity, and therefore, declines in trabecular bone volume were driven by decreased mechanical demands.⁽⁵⁾ It is also possible that an age-related accumulation of adipocytes in the marrow contributed to the age-related decline in BV/TV in adulthood. However, the relationship between an age-related accumulation of total body

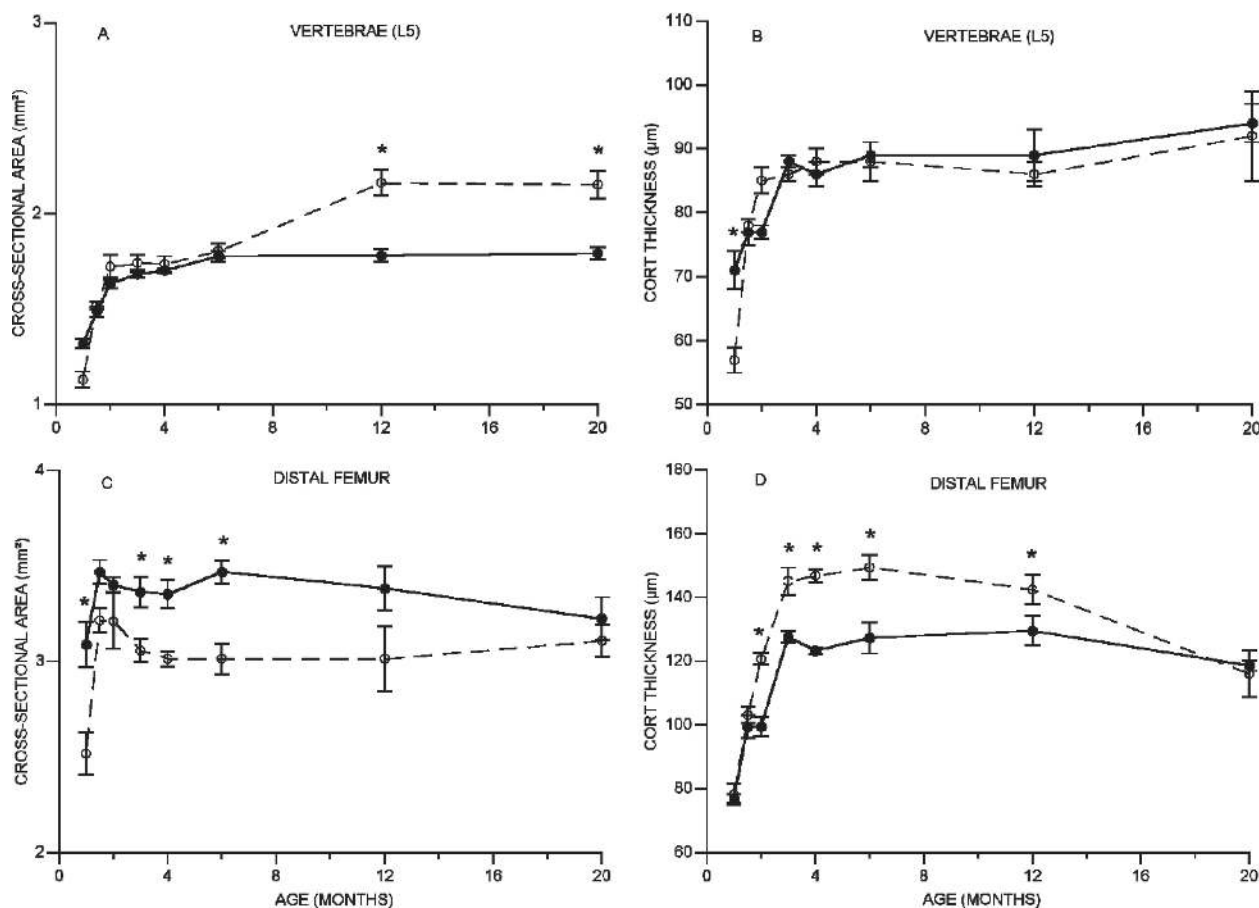


FIG. 5. Changes in bone CSA and cortical thickness at the vertebral body and distal femur in male and female mice from 1 to 20 mo of age, assessed by μ CT (mean \pm SE). Males are represented by solid symbol and line, whereas females are shown as open symbol and dashed line. *Difference between males and females at a given age ($p < 0.05$).

fat and marrow fat is poorly defined and deserves further study.^(31,34,35)

We noted that age-related changes in trabecular bone were more extensive in the appendicular skeleton than in the vertebral body (Table 1; Figs. 3 and 4). This observation seems counterintuitive to the presumed mechanical loading patterns associated with quadrupedal locomotion. To explain it, one must speculate about the possible function of trabecular bone in general and how these functions vary by skeletal site. We suggest that trabecular bone is needed for structural reasons: (1) to transmit forces from the joint surface to the cortex (the primary structural feature in long bones) and (2) in the epiphysis, to provide support to the subchondral bone and cartilage surface. The observation of greater age-related changes in the long bone metaphysis than in the vertebral body may be attributable to several factors. First, this observation suggests that mechanical forces are efficiently transmitted to the cortex of the long bones and that metaphyseal trabecular bone (i.e., in the secondary spongiosa) is not needed for mechanical function in mice, because despite early and marked declines in trabecular bone volume, the mice do not suffer spontaneous fractures. We note (but do not report quantitatively) that

age-related changes in trabecular bone in the epiphysis are minimal (see Fig. 4). Thus, it seems that trabecular bone is required in close proximity to the joint surface, and it is not required in the region of secondary spongiosa. Following this logic, we would speculate that load-transfer characteristics are different in the vertebral body and that a higher fraction of the loads is carried by the trabecular bone.⁽³⁶⁾ We hypothesize that this difference in load-transfer characteristics between the two skeletal sites contributes to the difference in patterns of age-related trabecular bone changes.

Our observation of an early peak and immediate decline in trabecular bone volume contrasts with a previous report in several inbred mouse strains showing that peak total femoral volumetric BMD, a measurement largely influenced by cortical bone, occurs at 4 mo of age and is relatively stable until 1 yr of age.⁽⁶⁾ It is not necessarily surprising, but perhaps underappreciated, that the timing of "peak" bone mass acquisition differs for trabecular and cortical compartments. Moreover, our data reinforce the notion that bone modeling and remodeling have different age-patterns on periosteal, endocortical, and trabecular surfaces.^(2,4)

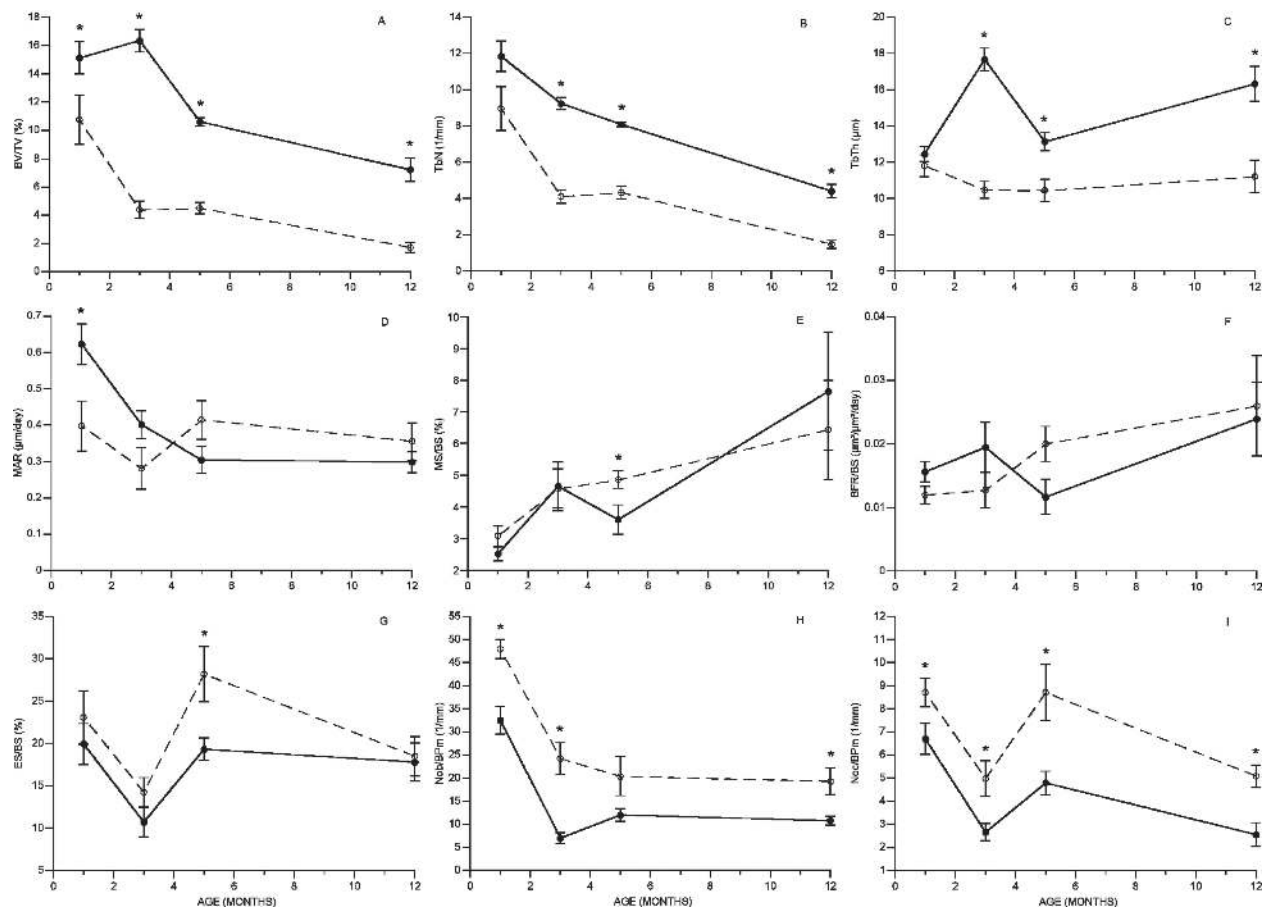


FIG. 6. Changes in trabecular bone architecture and indices of bone turnover at the distal femoral metaphysis in male and female C57Bl/6J mice from 1 to 12 mo of age, assessed by histomorphometry (mean \pm SE). Males are represented by solid symbol and line, whereas females are shown as open symbol and dashed line. *Difference between males and females at a given age ($p < 0.05$).

Previous studies in mice showed continued periosteal expansion with aging at mid-diaphyseal regions,^(1,2,4) a phenomena that would help to maintain whole bone bending strength in the face of endocortical resorption and declining material properties with age. However, our data are equivocal as to whether changes in cross-sectional geometry and/or cortical thickness ameliorate the anticipated declines in bone strength caused by loss of trabecular bone at the vertebral body and distal femoral metaphyseal regions. At these regions, dramatic gains in cross-sectional area occurred during the rapid phase of growth, but thereafter, there were no substantial increases in cross-sectional area, particularly at the distal femur, despite ongoing loss of trabecular bone volume. Thickness of the ventral vertebral cortex increased rapidly during growth and continued to increase, albeit slowly, throughout life, possibly helping to maintain vertebral compressive and bending strength. In contrast, at the distal femoral metaphysis, cortical thickness peaked at 3 mo of age and was either steady (in males) or declined (in females). The compensatory changes are difficult to interpret completely, because we did not yet assess bone matrix properties or perform mechanical testing, and thus we cannot ascertain how the changes we observed im-

pact bone fragility. It is likely that increased cross-sectional geometry and cortical thickness in adolescence compensates at least in part for declines in trabecular bone volume, although direct mechanical testing is needed to test this hypothesis.^(37,38)

Knowledge of age-related changes in trabecular bone of rodents is key for interpreting therapeutic and genetic interventions. Our data indicate that, unlike rats, who have a prolonged period of stable or even increasing trabecular bone volume at the lumbar spine and proximal tibia during adulthood (i.e., from 3 to 12 mo of age),⁽³⁹⁻⁴²⁾ during normal aging in mice, trabecular bone volume declines continuously after 2 mo of age. Although there is variability with age and skeletal site, trabecular bone remodeling rates, assessed by dynamic histomorphometry, are generally 2- to 3-fold higher in mice than rats, which may contribute to their higher rate of trabecular bone changes with age.^(9,22,43-51)

Age-related changes in humans are similar to those observed in mice. A recent population-based, cross-sectional study of men and women 21-97 yr of age examined bone microarchitecture at the distal radius using high-resolution 3D pQCT.⁽⁵²⁾ Similar to our findings in mice, young women

had lower trabecular BV/TV than men, and with aging, women had a greater decline in trabecular number than men.⁽⁵²⁾ Moreover, the age-related declines in BV/TV at the distal radius began in young adulthood, at a time of “normal” sex steroid levels, and were more pronounced in women than men. QCT-assessed trabecular volumetric BMD at the spine and proximal femur also showed a greater decrease over life in women than men.⁽⁵³⁾ Other studies have also shown age-related declines in volumetric BMD in the axial skeleton in young adults.^(54,55) Overall, the similar patterns of age-related changes in trabecular bone between humans and mice suggest that mice may be useful for studying the factors that contribute to the trabecular bone loss that occurs when sex steroid levels are normal.

A primary shortcoming of our study is that we infer age-related changes from a cross-sectional study. New in vivo μ CT systems will facilitate longitudinal assessment of changes in bone architecture with aging.^(56–58) In addition, further exploration of age-related changes in hormonal and cytokine profiles, as well as gene expression patterns, would help to delineate biologic and molecular mechanisms underlying the age-related changes that we observed. Finally, we only examined a single inbred strain and patterns of age-related change in bone microarchitecture may differ in other strains. Nonetheless, the strain we examined is widely used in biomedical research, and the data provided are critical for design and interpretation of experiments in skeletal biology.

In summary, our results indicate that age-related changes in vertebral, femoral, and tibial trabecular microarchitecture in mice occur early and continue throughout life. Many aspects of trabecular architecture differed between sexes at the time of peak trabecular bone volume acquisition, and in addition, the age-related deterioration was more pronounced in the metaphyseal regions of the long bones than in the vertebral body and was greater in females than males. Altogether, our findings provide strong rationale for further study of the interactions among sex-steroids and bone remodeling in inbred strains of mice to gain insights into the pathogenesis of skeletal fragility.

ACKNOWLEDGMENTS

Funding for this project was provided by National Institute of Health Grants AR0492265 (MLB), DK42424 (EC), and DK45227 (EC). The authors thank Laurie Green and Joshua Evans for assistance with μ CT measurements.

REFERENCES

1. Brodt MD, Ellis CB, Silva MJ 1999 Growing C57BL/6 mice increase whole bone mechanical properties by increasing geometric and material properties. *J Bone Miner Res* **14**:2159–2166.
2. Ferguson VL, Ayers RA, Bateman TA, Simske SJ 2003 Bone development and age-related bone loss in male C57BL/6J mice. *Bone* **33**:387–398.
3. Somerville JM, Aspden RM, Armour KE, Armour KJ, Reid DM 2004 Growth of C57BL/6 mice and the material and mechanical properties of cortical bone from the tibia. *Calcif Tissue Int* **74**:469–475.
4. Price C, Herman BC, Lufkin T, Goldman HM, Jepsen KJ 2005 Genetic variation in bone growth patterns defines adult mouse bone fragility. *J Bone Miner Res* **20**:1983–1991.
5. Hamrick MW, Ding KH, Pennington C, Chao YJ, Wu YD, Howard B, Immel D, Borlongan C, McNeil PL, Bollag WB, Curl WW, Yu J, Isaacs CM 2006 Age-related loss of muscle mass and bone strength in mice is associated with a decline in physical activity and serum leptin. *Bone* **39**:845–853.
6. Beamer WG, Donahue LR, Rosen CJ, Baylink DJ 1996 Genetic variability in adult bone density among inbred strains of mice. *Bone* **18**:397–403.
7. Halloran BP, Ferguson VL, Simske SJ, Burghardt A, Venton LL, Majumdar S 2002 Changes in bone structure and mass with advancing age in the male C57BL/6J mouse. *J Bone Miner Res* **17**:1044–1050.
8. Bouxsein ML, Myers KS, Shultz KL, Donahue LR, Rosen CJ, Beamer WG 2005 Ovariectomy-induced bone loss varies among inbred strains of mice. *J Bone Miner Res* **20**:1085–1092.
9. Bouxsein ML, Pierroz DD, Glatt V, Goddard DS, Cavat F, Rizzoli R, Ferrari SL 2005 beta-Arrestin2 regulates the differential response of cortical and trabecular bone to intermittent PTH in female mice. *J Bone Miner Res* **20**:635–643.
10. Judex S, Garman R, Squire M, Busa B, Donahue LR, Rubin C 2004 Genetically linked site-specificity of disuse osteoporosis. *J Bone Miner Res* **19**:607–613.
11. Ridler T, Calvard S 1978 Picture thresholding using an iterative selection method. *IEEE Trans Syst Man Cybern SMC* **8**:630–632.
12. Meinel L, Fajardo R, Hofmann S, Langer R, Chen J, Snyder B, Vunjak-Novakovic G, Kaplan D 2005 Silk implants for the healing of critical size bone defects. *Bone* **37**:688–698.
13. Rajagopalan S, Lu L, Yaszemski MJ, Robb RA 2005 Optimal segmentation of microcomputed tomographic images of porous tissue-engineering scaffolds. *J Biomed Mater Res A* **75**:877–887.
14. Hildebrand T, Laib A, Muller R, Dequeker J, Rueggsegger P 1999 Direct three-dimensional morphometric analysis of human cancellous bone: Microstructural data from spine, femur, iliac crest, and calcaneus. *J Bone Miner Res* **14**:1167–1174.
15. Hildebrand T, Rueggsegger P 1997 A new method for the model independent assessment of thickness in three-dimensional images. *J Microsc* **185**:67–75.
16. Hildebrand T, Rueggsegger P 1997 Quantification of bone microarchitecture with the structure model index. *Comp Method Biomech Biomed Eng* **1**:5–23.
17. Gazerro E, Pereira RC, Jorgetti V, Olson S, Economides AN, Canalis E 2005 Skeletal overexpression of gremlin impairs bone formation and causes osteopenia. *Endocrinology* **146**:655–665.
18. Parfitt A, Drezner M, Glorieux F, Kanis J, Recker R 1987 Bone histomorphometry: Standardization of nomenclature, symbols and units. *J Bone Miner Res* **2**:595–610.
19. Ruimerman R, Hilbers P, van Rietbergen B, Huiskes R 2005 A theoretical framework for strain-related trabecular bone maintenance and adaptation. *J Biomech* **38**:931–941.
20. Parikka V, Peng Z, Hentunen T, Risteli J, Elo T, Vaananen HK, Harkonen P 2005 Estrogen responsiveness of bone formation in vitro and altered bone phenotype in aged estrogen receptor-alpha-deficient male and female mice. *Eur J Endocrinol* **152**:301–314.
21. Rulli SB, Huhtaniemi I 2005 What have gonadotrophin over-expressing transgenic mice taught us about gonadal function? *Reproduction* **130**:283–291.
22. Oz OK, Zerwekh JE, Fisher C, Graves K, Nanu L, Millsaps R, Simpson ER 2000 Bone has a sexually dimorphic response to aromatase deficiency. *J Bone Miner Res* **15**:507–514.
23. Miyaura C, Toda K, Inada M, Ohshiba T, Matsumoto C, Okada T, Ito M, Shizuta Y, Ito A 2001 Sex- and age-related response to aromatase deficiency in bone. *Biochem Biophys Res Commun* **280**:1062–1068.
24. Cao J, Venton L, Sakata T, Halloran BP 2003 Expression of RANKL and OPG correlates with age-related bone loss in male C57BL/6 mice. *J Bone Miner Res* **18**:270–277.

25. Cao JJ, Wronski TJ, Iwaniec U, Phleger L, Kurimoto P, Boudignon B, Halloran BP 2005 Aging increases stromal/osteoblastic cell-induced osteoclastogenesis and alters the osteoclast precursor pool in the mouse. *J Bone Miner Res* **20**:1659–1668.
26. Pfeilschifter J 2003 Role of cytokines in postmenopausal bone loss. *Curr Osteoporos Rep* **1**:53–58.
27. Varanasi SS, Francis RM, Berger CE, Papiha SS, Datta HK 1999 Mitochondrial DNA deletion associated oxidative stress and severe male osteoporosis. *Osteoporos Int* **10**:143–149.
28. Ozgocmen S, Kaya H, Fadilioglu E, Aydogan R, Yilmaz Z 2007 Role of antioxidant systems, lipid peroxidation, and nitric oxide in postmenopausal osteoporosis. *Mol Cell Biochem* **295**:45–52.
29. Reid IR 2002 Relationships among body mass, its components, and bone. *Bone* **31**:547–555.
30. Reid IR 2004 Leptin deficiency—lessons in regional differences in the regulation of bone mass. *Bone* **34**:369–371.
31. Meunier P, Aaron J, Edouard C, Vignon G 1971 Osteoporosis and the replacement of cell populations of the marrow by adipose tissue. A quantitative study of 84 iliac bone biopsies. *Clin Orthop* **80**:147–154.
32. Richard S, Torabi N, Franco GV, Tremblay GA, Chen T, Vogel G, Morel M, Cleroux P, Forget-Richard A, Komarova S, Tremblay ML, Li W, Li A, Gao YJ, Henderson JE 2005 Ablation of the Sam68 RNA binding protein protects mice from age-related bone loss. *PLoS Genet* **1**:e74.
33. Rosen CJ, Bouxsein ML 2006 Mechanisms of Disease: Is osteoporosis the obesity of bone? *Nat Clin Pract Rheumatol* **2**:35–43.
34. Justesen J, Stenderup K, Ebbesen EN, Mosekilde L, Steiniche T, Kassem M 2001 Adipocyte tissue volume in bone marrow is increased with aging and in patients with osteoporosis. *Biogerontology* **2**:165–171.
35. Verma S, Rajaratnam JH, Denton J, Hoyland JA, Byers RJ 2002 Adipocytic proportion of bone marrow is inversely related to bone formation in osteoporosis. *J Clin Pathol* **55**:693–698.
36. Tommasini SM, Morgan TG, van der Meulen M, Jepsen KJ 2005 Genetic variation in structure-function relationships for the inbred mouse lumbar vertebral body. *J Bone Miner Res* **20**:817–827.
37. van der Meulen MC, Jepsen KJ, Mikic B 2001 Understanding bone strength: Size isn't everything. *Bone* **29**:101–104.
38. Jarvinen TL, Sievanen H, Jokihaara J, Einhorn TA 2005 Revival of bone strength: The bottom line. *J Bone Miner Res* **20**:717–720.
39. Wronski TJ, Dann LM, Horner SL 1989 Time course of vertebral osteopenia in ovariectomized rats. *Bone* **10**:295–301.
40. Barbier A, Martel C, de Vernejoul MC, Tirode F, Nys M, Mocaer G, Morieux C, Murakami H, Lacheretz F 1999 The visualization and evaluation of bone architecture in the rat using three-dimensional X-ray microcomputed tomography. *J Bone Miner Metab* **17**:37–44.
41. Li XJ, Jee WS, Chow SY, Woodbury DM 1990 Adaptation of cancellous bone to aging and immobilization in the rat: A single photon absorptiometry and histomorphometry study. *Anat Rec* **227**:12–24.
42. Wang L, Banu J, McMahan CA, Kalu DN 2001 Male rodent model of age-related bone loss in men. *Bone* **29**:141–148.
43. Sims NA, Dupont S, Krust A, Clement-Lacroix P, Minet D, Resche-Rigon M, Gaillard-Kelly M, Baron R 2002 Deletion of estrogen receptors reveals a regulatory role for estrogen receptors-beta in bone remodeling in females but not in males. *Bone* **30**:18–25.
44. Ke HZ, Qi H, Chidsey-Frink KL, Crawford DT, Thompson DD 2001 Lasofoxifene (CP-336,156) protects against the age-related changes in bone mass, bone strength, and total serum cholesterol in intact aged male rats. *J Bone Miner Res* **16**:765–773.
45. Nishida S, Okimoto N, Okazaki Y, Yamaguchi A, Kumegawa M, Yasukawa K, Murayama K, Nakamura T 1998 Effect of monoclonal anti-human gp130 antibody (GPX7) on bone turnover in normal and ovariectomized rats. *Calcif Tissue Int* **62**:227–236.
46. Akhter MP, Otero JK, Iwaniec UT, Cullen DM, Haynatzki GR, Recker RR 2004 Differences in vertebral structure and strength of inbred female mouse strains. *J Musculoskelet Neuronal Interact* **4**:33–40.
47. Lane NE, Yao W, Kinney JH, Modin G, Balooch M, Wronski TJ 2003 Both hPTH(1-34) and bFGF increase trabecular bone mass in osteopenic rats but they have different effects on trabecular bone architecture. *J Bone Miner Res* **18**:2105–2115.
48. Iida-Klein A, Zhou H, Lu SS, Levine LR, Ducayen-Knowles M, Dempster DW, Nieves J, Lindsay R 2002 Anabolic action of parathyroid hormone is skeletal site specific at the tissue and cellular levels in mice. *J Bone Miner Res* **17**:808–816.
49. Hefferan TE, Evans GL, Lotinun S, Zhang M, Morey-Holton E, Turner RT 2003 Effect of gender on bone turnover in adult rats during simulated weightlessness. *J Appl Physiol* **95**:1775–1780.
50. Lotinun S, Limlomwongse L, Sirikulchayanonta V, Krishnamra N 2003 Bone calcium turnover, formation, and resorption in bromocriptine- and prolactin-treated lactating rats. *Endocrine* **20**:163–170.
51. David V, Lafage-Proust MH, Laroche N, Christian A, Rueggsegger P, Vico L 2006 Two-week longitudinal survey of bone architecture alteration in the hindlimb-unloaded rat model of bone loss: Sex differences. *Am J Physiol Endocrinol Metab* **290**:E440–E447.
52. Khosla S, Riggs BL, Atkinson EJ, Oberg AL, McDaniel LJ, Holets M, Peterson JM, Melton LJ III 2006 Effects of sex and age on bone microstructure at the ultradistal radius: A population-based noninvasive in vivo assessment. *J Bone Miner Res* **21**:124–131.
53. Riggs BL, Melton LJ III, Robb RA, Camp JJ, Atkinson EJ, Peterson JM, Rouleau PA, McCollough CH, Bouxsein ML, Khosla S 2004 Population-based study of age and sex differences in bone volumetric density, size, geometry, and structure at different skeletal sites. *J Bone Miner Res* **19**:1945–1954.
54. Meier DE, Orwoll ES, Keenan EJ, Fagerstrom RM 1987 Marked decline in trabecular bone mineral content in healthy men with age: Lack of association with sex steroid levels. *J Am Geriatr Soc* **35**:189–197.
55. Yu W, Qin M, Xu L, van Kuijk C, Meng X, Xing X, Cao J, Genant HK 1999 Normal changes in spinal bone mineral density in a Chinese population: Assessment by quantitative computed tomography and dual-energy X-ray absorptiometry. *Osteoporos Int* **9**:179–187.
56. Waarsing JH, Day JS, van der Linden JC, Ederveen AG, Spanjers C, De Clerck N, Sasov A, Verhaar JA, Weinans H 2004 Detecting and tracking local changes in the tibiae of individual rats: A novel method to analyse longitudinal in vivo micro-CT data. *Bone* **34**:163–169.
57. Waarsing JH, Day JS, Verhaar JA, Ederveen AG, Weinans H 2006 Bone loss dynamics result in trabecular alignment in aging and ovariectomized rats. *J Orthop Res* **24**:926–935.
58. Boyd SK, Davison P, Muller R, Gasser JA 2006 Monitoring individual morphological changes over time in ovariectomized rats by in vivo micro-computed tomography. *Bone* **39**:854–862.

Address reprint requests to:

Mary L Bouxsein, PhD

Orthopedic Biomechanics Laboratory, RN 115

Beth Israel Deaconess Medical Center

330 Brookline Avenue

Boston, MA 02215, USA

E-mail: mbouxsei@bidmc.harvard.edu

Received in original form October 11, 2006; revised form April 17, 2007; accepted May 2, 2007.